A Comprehensive Toolkit for Semi-Automated HD Maps Production: Integrating AI-Driven Feature Extraction with 3D Interactive Validation and Editing

Yi-Feng Chang [1, a] *, Kai-Wei Chiang [1, b], Meng-Lun Tsai [1, c], Pei-Ling Lee [1, d], Syun Tsai [1, e], Chi-Hsin Huang [1, f], Ting-Chun Wu [1, g], Yi-Han Jen [1, h], Jiun-Yo Lin [1, i], Chang-Le Lee [1, j], Ching-Hsiang Lin [1, k], Han-Che Huang [1, l]

[1] NCKU, Department of Geomatics, No. 1, Daxue Rd., East Dist., Tainan City 701401, Taiwan – [a] F64066185@gs.ncku.edu.tw, [b] kwchiang@geomatics.ncku.edu.tw, [c] taurusbryant@geomatics.ncku.edu.tw, [d] pointlpl@geomatics.ncku.edu.tw, [e] dino920135@gmail.com, [f] a56096609@gmail.com, [g] easy3123@gmail.com, [h] f64084028@gs.ncku.edu.tw, [i] f64091122@gs.ncku.edu.tw, [j] p68141504@gs.ncku.edu.tw, [k] seanlin151@gmail.com, [l] 11206026@gs.ncku.edu.tw

Keywords: High-definition Maps, Mobile Laser Scanning, Semi-automatic Algorithm, AI-driven Feature Extraction, Human-in-the-loop Toolchain.

ABSTRACT:

This paper presents a comprehensive toolkit for semi-automated High-Definition Maps (HD Maps) production that integrates Artificial Intelligence (AI)-driven feature extraction with 3D human-in-the-loop validation. High-definition maps provide centimeter-level road geometry and traffic asset information, but large-scale production remains costly due to dense mobile mapping data and manual digitization. The proposed workflow consists of two self-developed components: a Semi-automated HD Maps Production Tool for batch extraction and a 3D HD Maps Validation and Editing Tool for structured review. The project-based pipeline ingests georeferenced mobile laser scanning point clouds, Inertial Navigation System / Global Navigation Satellite System (INS/GNSS) trajectories, and camera imagery, and applies configurable chains of ground filtering, road-marking extraction, voxel down-sampling, clustering, oriented bounding box analysis, and AI-based traffic asset detection. Candidate features with confidence indicators and basic attributes are stored in a project database and edited in a tightly coupled 3D environment that supports snapping, constrained adjustments, and semantic reclassification while logging all user edits. The toolkit is evaluated on a closed proving ground (CARLab, Shalun) and a freeway section of Taiwan National Highway No. 3. At CARLab, semi-automated extraction achieves F1-scores of 0.85–0.95 for key layers. For a one-kilometer highway section, operator time is reduced from 90–120 minutes in a purely manual Geographic Information System (GIS) workflow to about 45 minutes with the proposed approach, while maintaining comparable geometric accuracy. These results demonstrate a practical path towards scalable, traceable HD Maps production for autonomous driving applications.

1. INTRODUCTION

1.1 The Cost Problem in HD Maps Production

High-definition maps (HD Maps) encode centimeter-level lane geometry, road topology, and traffic-control asset information critical for autonomous driving localization, prediction, and planning (Elghazaly et al., 2023; Wong et al., 2021). While representational standards such as shapefiles, Lanelet2 and OpenDRIVE have matured, the production pipelines that generate these maps remain fragmented and costly (Chiang et al., 2022; Liu et al., 2024).

A conventional production cycle threads through at least four distinct software environments: a LiDAR processing suite for ground filtering, a deep-learning framework for image-based detection, a 2D GIS platform for manual digitization, and a format-conversion utility for export. Each handoff requires format translation, coordinate alignment, and operator familiarity with a different interface.

Previous research has advanced individual pipeline components, Cloth Simulation Filter (CSF) ground filtering (Zhang et al., 2016), intensity-based marking extraction (Chang, 2023), oriented bounding box (OBB) classification (Gottschalk et al., 2000), and Mask Region-based Convolutional Neural Network (Mask R-CNN) detection (He et al., 2017). Existing studies have advanced individual components; however, end-to-end production integration remains less discussed (Liu et al., 2024).

This paper presents a self-developed toolchain that addresses this gap through two coupled applications: (1) a semi-automated HD Maps production tool with a dual-path extraction pipeline (One path for road surface markings, another path for non-ground traffic assets); and (2) a 3D HD Maps validation and editing tool that goes beyond conventional review. The fundamental distinction from prior work lies in the system-level integration: formalizing the algorithmic–human boundary, eliminating cross-platform processing.

1.2 Contribution

The proposed self-developed toolchain designed around a clear principle: machines should generate candidate features through batch processing; humans should provide quality-critical judgment through structured review. The toolchain comprises two applications:

(1) A self-developed semi-automated HD Maps production tool that generates initial vector maps. This tool integrates Inertial Navigation System / Global Navigation Satellite System (INS/GNSS) navigation trajectories, LiDAR point clouds, high-resolution camera imagery, Convolutional Neural Network (CNN)-based object detection, and a Vision-Language Model (VLM) for classification assistance into extraction pipeline.

(2) A self-developed three-dimensional (3D) HD Maps validation and editing tool where operators import the initial vector maps, perform fine-tuning and review in an interactive 3D point-cloud environment, and export the validated result as publishable shapefiles.

2. METHODOLOGY

Figure 1 shows the complete workflow architecture. Data flows from the mobile mapping system into the production tool, which generates initial vector maps via a dual-path pipeline; these initial vector maps are then imported into the 3D editing tool for human review, fine-tuning, and attribute confirmation; the validated output is exported as publishable shapefiles.

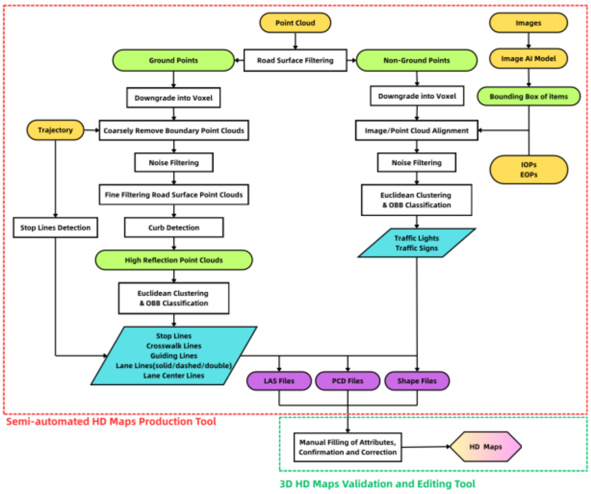

Figure 1. Architecture of the self-developed semi-automated HD Maps production toolchain.

2.1 Data Acquisition

The toolchain imports three synchronised data streams collected by the mobile mapping system reported by Zeng (2020), as shown in Figure 2: georeferenced LiDAR point clouds, INS/GNSS navigation trajectories, and high-resolution camera images. The 3D coordinates of each LiDAR point in the mapping frame are determined by the direct georeferencing equation (Chiang et al., 2022):

$$r_m = r_{b(t)} + R_n^{b(t)} \cdot [R_b^s \cdot r_s + l_b^s] \tag{1}$$

where r_m denotes the point position in the mapping coordinate frame; $r_{b(t)}$ is the position of the INS/GNSS body frame at time t; $R_n^{b(t)}$ is the rotation matrix transforming from the body frame to the navigation frame; R_b^s is the boresight rotation from the LiDAR scanner frame to the body frame; r_s is the range vector measured by the LiDAR scanner; and l_b^s is the lever-arm offset between the scanner origin and the INS centre. Accurate calibration of the boresight and lever-arm parameters is essential for achieving the centimeter-level accuracy required by HD Maps.

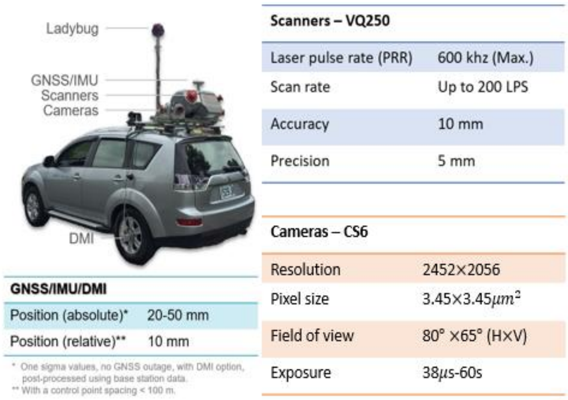

Figure 2. Mobile mapping system (Zeng, 2020).

2.2 Semi-automated HD Maps Production Tool

The toolkit is implemented as a project-based application that imports synchronised multi-sensor data from mobile mapping platforms, including georeferenced LiDAR point clouds, GNSS/INS trajectories, and camera imagery (Chiang et al., 2022; Ma et al., 2019). Within each project, road segments are organized as jobs with defined regions of interest and configuration parameters.

Users define processing profiles that specify semi-automated extraction pipelines. Existing modules for ground filtering, high-intensity road marking extraction, voxel down-sampling, euclidean clustering, OBB analysis, and AI-based detection of traffic assets are arranged into configurable chains. These pipelines support batch extraction of lane markings, lane center lines, stop lines, guiding lines, crosswalk lines, traffic signs and traffic lights. Heavy pre-processing steps (e.g., ground filtering and clustering) can be cached and reused when parameters are adjusted, enabling iterative tuning without re-running the full computation. The Graphical User Interface (GUI) of semi-automated HD Maps production tool as shown in Figure 3.

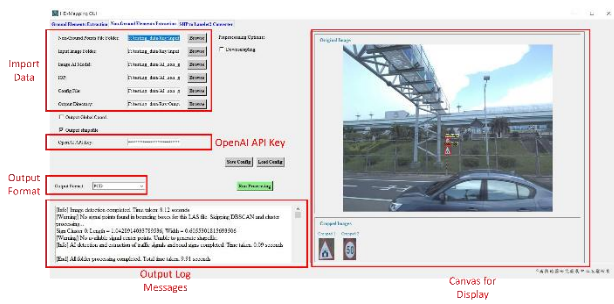

Figure 3. GUI of the semi-automated HD Maps production tool.

2.2.1 Path A: Road Surface Marking Extraction

The raw point cloud is first separated into ground points and non-ground points using the CSF proposed by Zhang et al. (2016). Unlike traditional filtering methods based on elevation thresholds, CSF simulates a rigid cloth falling under gravity over the inverted point cloud.

The ground point cloud then undergoes voxel downsampling to reduce data density while preserving geometric features. The 3D space is partitioned into a regular grid of cubic voxels with edge length v = 0.05 m; within each voxel V_k, all contained points are replaced by their centroid:

$$\bar{p}_k = (1/N_k)\sum p_i \text{, for all } i \in V_k \quad (2)$$

where N_k is the number of points within voxel V_k, and p_i are the individual point coordinates. Additional preprocessing includes trajectory-assisted boundary removal (discarding points beyond a configurable lateral distance from the vehicle trajectory to eliminate roadside clutter), statistical outlier removal, and curb detection based on local elevation gradients (Yang et al., 2013).

To separate painted road markings from the asphalt surface, Otsu’s thresholding method (Otsu, 1979) is applied to the intensity histogram of the ground point cloud. This method determines an optimal threshold by maximising the between-class variance σ_B^2:

$$\sigma_B^2(t) = \omega_0(t) \cdot \omega_1(t) \cdot [\mu_0(t) - \mu_1(t)]^2 \quad (3)$$

where $\omega_0(t)$ and $\omega_1(t)$ are the class probabilities of asphalt and paint at threshold t, and $\mu_0(t)$ and $\mu_1(t)$ are their respective mean intensity values. This automated approach adapts to varying surface conditions without manual threshold selection.

The resulting high-reflectivity points are grouped into spatially coherent clusters using Euclidean distance-based clustering (Rusu, 2010). Each cluster is then characterised by an Oriented Bounding Box (OBB) computed via Principal Component Analysis (PCA) on the 2D projected coordinates (Gottschalk et al., 2000; Jiang, 2017). The covariance matrix C of a cluster with n points is:

$$C = (1/n)\sum(p_i - \bar{p})(p_i - \bar{p})^T \quad (4)$$

where $\bar{p}$ is the cluster centroid. The eigenvectors e_1 and e_2 of C define the principal axes of the OBB. The length L and width W of the bounding box are computed as the extent of point projections along these axes:

$$L = max(p_i \cdot e_1) - min(p_i \cdot e_1) \quad (5a)$$

$$W = max(p_i \cdot e_2) - min(p_i \cdot e_2) \quad (5b)$$

A rule-based classifier then assigns each cluster to a road marking category based on its geometric properties(L, W), the aspect ratio L/W, and against road marking design standards published by Taiwan’s Ministry of Transportation and Communications (MOTC). The classification thresholds are summarised in Table 1.

Table 1. OBB classification thresholds calibrated to Taiwan MOTC road marking design standards.

Feature type	L/W	W (m)
Lane line	-	0.10–0.25
Crosswalk line	1–5	0.30–0.60
Stop line	< 3	> 2.5
Guiding line	1–4	0.30–1.50

2.2.2 Path B: Traffic Light and Traffic Sign Extraction

Path B simultaneously processes non-ground points and camera images to detect and localize traffic lights and traffic signs. Camera images are processed by a CNN detection model, specifically, Mask R-CNN (He et al., 2017) built on a Faster Region-based CNN (Faster R-CNN) backbone (Ren et al., 2015) with a Feature Pyramid Network (FPN) for multi-scale feature extraction (Lin et al., 2017). The model generates bounding boxes and instance segmentation masks for each detected traffic asset. Additionally, a VLM is employed to refine detection results and provide semantic classification assistance—for example, distinguishing between regulatory, warning, and informational sign types based on visual content analysis.

To achieve precise spatial integration between 2D image detections and the 3D point cloud, the detected bounding boxes are projected into the point-cloud coordinate system using the Exterior Orientation Parameters (EOPs), the camera position and attitude at the instant of image capture, derived from the synchronised INS/GNSS trajectory and the camera-to-body extrinsic calibration. A 3D view corresponding to each 2D bounding box is constructed in the point-cloud space, and non-ground points within each view are extracted as candidate traffic-asset clusters as shown in Figure 4. Noise filtering is applied to isolate the traffic-asset structure from irrelevant points, and the 3D centroid of each refined cluster is computed to serve as the spatial reference position in the output HD Maps layer.

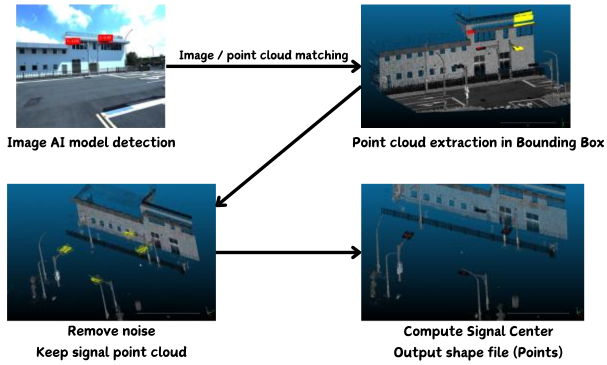

Figure 4. Image detection, EOP-based alignment, and 3D point-cloud fusion for traffic asset extraction.

2.3 Output and Format Support

Both paths converge at the output stage. Proposed production tool exports extracted features in three formats: LAS point-cloud files preserving the full-resolution classified point cloud, Point Cloud Data (PCD) files for compatibility with 3D visualisation tools, and shapefiles storing vector-based features with semantic attributes for GIS integration. All three formats are generated from the same internal representation, ensuring geometric and attribute consistency.

2.4 Evaluation Metrics

Extraction performance is quantified using precision (P), recall (R), and F1-score (Powers, 2011), defined as:

$$P = \frac{TP}{TP+FP};\ R = \frac{TP}{TP+FN};\ F1 = \frac{2PR}{P+R} \quad (6)$$

where TP denotes the number of correctly extracted features (true positives), FP the number of incorrectly extracted features (false positives), and FN the number of features present in the ground truth but missed by the algorithm (false negatives). Ground truth was established by expert manual annotation of the test-site point clouds.

2.5 3D HD Maps Validation and Editing Tool

Figure 5. GUI of the 3D HD Maps validation and editing tool.

The second component of the toolchain is a self-developed 3D HD Maps validation and editing tool, designed to serve as the human-in-the-loop stage of the production workflow. The GUI as shown in Figure 5. Its purpose is to import the initial vector maps generated by the semi-automated HD Maps production tool, enable operators to fine-tune and review every extracted feature in an interactive 3D environment, and export the validated result as publishable shapefiles.

The tool renders all candidate features as editable vector primitives overlaid on the original or processed point cloud and vehicle trajectory. Operators navigate the scene via orbit, pan, and zoom controls, and can selectively toggle individual feature layers (e.g., lane lines, stop lines, traffic signs) to focus on specific elements during review. The editing workflow is structured into three sub-tasks:

(a) Confirmation: operators review each initial vector map against the 3D point cloud and confirm correct extractions. In our evaluations, approximately 85% of candidates required no modification, meaning the operator's cognitive load is primarily verification rather than creation.

(b) Correction: misclassified or geometrically inaccurate features are corrected using constrained editing operations. Vertex snapping attracts edited vertices to the nearest point-cloud geometry, preventing features from drifting off the road surface.

(c) Attribute confirmation: operators confirm semantic attributes such as marking subtype, lane assignment, and signal phase. This step bridges the gap between geometric extraction and semantic map content (what autonomous driving systems require).

3. RESULTS AND DISCUSSION

3.1 Test Sites

The toolchain was evaluated on two representative Mobile Laser Scanning (MLS) datasets:

3.1.1 Taiwan CARLab.

(1) Controlled Test Field:

The Taiwan CARLab, located in Shalun, Tainan, is a closed-field testing facility designed for autonomous driving research as shown in Figure 6. It features thirteen simulated traffic scenarios including railway crossings, curved roads, tunnels, roundabouts, and multi-lane intersections. The facility provides well-defined ground truth with clearly painted markings and standard traffic infrastructure and eliminates interference from real traffic.

Figure 6. Taiwan CARLab proving ground (CARTURE, 2019).

3.1.2 National Highway No. 3.

The second test site is a section of Taiwan's National Highway No. 3, chosen for its repetitive highway geometry representative of real-world road networks. This site introduces challenges absent in the controlled environment: varying road surface conditions, dynamic lighting, partial occlusions from other vehicles, and sensor noise from vehicle vibrations at highway speed.

3.2 Extraction Results

At CARLab, Path A mainly extracts stop lines, crosswalk lines, guiding lines, and lane lines from ground points, while Path B extracts traffic lights and traffic signs through image-based AI detection and 3D point-cloud fusion, as shown in Figures 7 and 8. In Figure 7, the red vectors represent extracted stop lines; the cyan vectors represent extracted crosswalk lines; the green vectors represent extracted guiding lines, and the white vectors represent extracted lane lines, overlaid on the point cloud to show their geometric alignment with the road surface. In Figure 8, the red points denote extracted traffic lights, and the blue points denote extracted traffic signs, allowing the spatial distribution of both asset classes to be inspected directly in 3D space. On National Highway No. 3, the extraction results are shown in Figure 9. White lines represent solid lane markings, yellow lines indicate dashed lane lines, green lines indicate double lane lines, and red lines denote the lane center lines. The proposed algorithm was able to extract these features without requiring large parameter readjustment relative to CARLab, demonstrating the system's cross-site transferability. This transferability is significant: these rules are based on national MOTC design standards rather than site-specific empirical fitting, thus ensuring inherent robustness across road types conforming to the same standards.

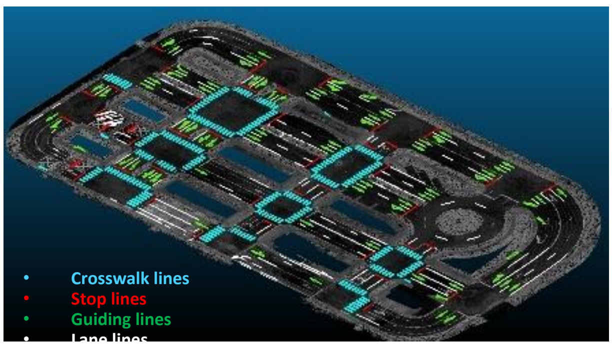

Figure 7. Path A extraction results at CARLab.

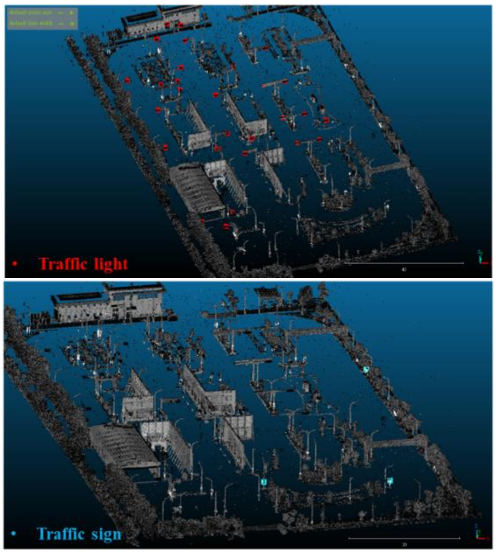

Figure 8. Path B results: traffic lights and signs at CARLab.

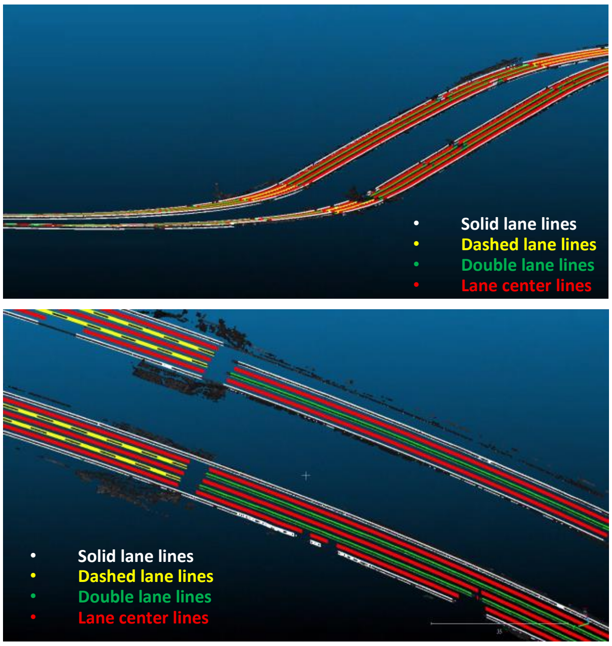

Figure 9. Extraction results on National Highway No. 3.

3.3 Validation and Editing Workflow in Practice

After batch extraction, operators loaded all initial vector maps into the 3D editing tool. The practical validation workflow comprised three stages: (1) Confirmation: correctly extracted features were confirmed via layer-wide review in the 3D viewer, where operators toggled each layer and visually inspected against the point cloud. At CARLab, approximately 85 % of extracted features required no modification. (2) Error correction: misclassified or geometrically inaccurate features were corrected using constrained editing. The most common corrections were extension of fragmented lane-line segments across scan gaps. (3) Attribute confirmation: For CARLab’s complex layout, approximately 85% of automatically generated attributes were correct; the remaining 15 % were manually adjusted.

At CARLab, the primary editing tasks were: (a) correcting misclassified clusters at complex intersections where geometric ambiguity is highest; (b) merging fragmented lane-line segments caused by occlusions or scan gaps; and (c) verifying traffic-asset centroids by comparing against the point cloud. The constrained editing tools especially vertex snapping and lane-aligned adjustment proved essential for maintaining geometric consistency; operators reported that these constraints prevented accidental misalignments that commonly occurred in unconstrained 2D GIS editing.

On Highway No. 3, the editing focus shifted to lane connectivity: ensuring that extracted lane-line vectors correctly link across segment boundaries, resolving gaps caused by vehicles partially occluding the road surface, and adjusting centerlines to follow the true road curvature.

3.4 Quantitative Evaluation

This section evaluates the proposed toolchain from three complementary perspectives: feature-level extraction quality, production efficiency, and system-level positioning against representative existing workflows. The first analysis focuses on CARLab, where the controlled environment provides reliable reference data for precision, recall, and F1-score assessment. The second analysis examines practical operator time on a 1-kilometer highway section, while the third contrasts the proposed framework with alternative production approaches in terms of integration, editing capability, and intelligence support.

3.4.1 Extraction Performance.

Table 2 summarises the extraction performance at CARLab. Overall, the results indicate that the proposed workflow achieves consistently high precision across all evaluated layers, ranging from 0.97 to 1.00, which means that most extracted candidates correspond to true road features or traffic assets. Crossing lines yield the highest F1-score (0.95), showing that this class is both geometrically distinctive and reliably detected under the controlled conditions of the proving ground. Stop lines and guiding lines also maintain high precision, but their comparatively lower recalls suggest that some instances remain partially missed, likely due to fragmentation, local intensity variation, or geometric ambiguity near intersections. For Path B, traffic lights and traffic signs both achieve perfect precision in this experiment, indicating that the combined image-based detection and 3D filtering strategy is effective at suppressing false positives; however, recall remains lower than for road-surface markings, especially for traffic signs, which implies that some assets are still missed during detection or point-cloud association. As for the highway dataset, the system automatically delineates dashed and solid lane lines and computes lane center lines. Using the 3D HD Maps validation and editing tool, operators then refine lane connectivity, resolve gaps caused by occlusions or partial scans, and ensure that the extracted vectors follow the true road alignment.

Table 2. Semi-automated extraction performance at CARLab proving ground

Layers	Precision	Recall	F1-score
Stop line	0.98	0.80	0.88
Crosswalk line	0.98	0.93	0.95
Guiding line	0.97	0.78	0.86
Traffic light	1.00	0.85	0.92
Traffic sign	1.00	0.75	0.86

3.4.2 Production Efficiency and Time-Saving Analysis.

Table 3 compares the conventional manual workflow, where an operator digitalizes all features in a 2D GIS environment, with the proposed toolchain for an average 1-kilometer highway section. The toolchain reduces total operator time from 90–120 minutes to approximately 45 minutes, corresponding to a 50–60% reduction. The automated extraction phase (approximately 25 minutes) runs largely unattended; the human phase (approximately 20 minutes) is spent in the 3D editing tool on confirmation, fine-tune, and correction.

Table 3. Comparison of manual and semi-automated HD Maps production time for an average 1-kilometer highway section.

Step	Manual (min)	Proposed (min)
Preprocessing + extraction	90–120	~ 25 (automated)
Validation / Fine-tune	(included above)	~ 20 (human)
Total time cost	**90–120**	**~ 45**

3.4.3 Comparison with Existing Approaches

Table 4 provides a qualitative comparison between the proposed toolchain and representative existing production approaches across four dimensions. The proposed toolchain is the only approach that offers end-to-end integration with built-in CNN+VLM detection, interactive 3D editing, and feature-level audit logging within a single workflow. Commercial tools such as RiPROCESS excel at point-cloud preprocessing but do not provide HD-Maps-specific classification, AI-based detection, or 3D validation editing. Script-based pipelines (QGIS + Python) offer flexibility but require manual data marshalling between tools and provide no audit trail.

Table 4. Qualitative comparison with existing HD Maps production approaches.

Criterion	Manual GIS	RiPROCESS	QGIS+scripts	Proposed
Integration	None	Partial	Loose	Full
3D editing	No	View only	2D only	Yes
AI detection	No	No	External	Built-in
VLM integration	No	No	No	Yes

4. CONCLUSIONS

This paper presents a human-in-the-loop toolchain for semi-automated HD Maps production that explicitly structures the division of labour between automated extraction and human quality assurance. The semi-automated HD Maps production tool integrates INS/GNSS navigation trajectories, LiDAR point clouds, camera imagery, CNN-based detection, and VLM-assisted classification into a dual-path extraction pipeline that generates initial vector maps. The 3D HD Maps validation and editing tool enables operators to fine-tune and review these initial vector maps in an interactive 3D environment.

Evaluations at the Taiwan CARLab and National Highway No. 3 demonstrate 50–60% reduction in total operator time compared with conventional manual digitization. The toolchain effectively addresses the two core pain points of current HD Maps production: high labour and time costs are reduced through automated batch extraction and cross-platform complexity is eliminated.

Future work will target: (1) multi-site evaluations across urban, suburban, and rural road shape environments to further validate generalization; (2) context-aware classification incorporating intersection proximity and road hierarchy to resolve geometric ambiguity at complex intersections; (3) multi-camera fusion and point-cloud-native detection models such as PointNet++(Qi et al., 2017) to improve traffic-asset recall; (4) distributed processing for corridors exceeding 100 km; and (5) expanded export format support including OpenDRIVE and Lanelet2.

REFERENCES

CARTURE. 政府一小步，台灣智慧駕駛科技一大步, 2019. Retrieved from https://www.carture.com.tw/topic/article/5663 (accessed 23 March 2026)

Chang, Y.-F., 2023. Semi-automated generation of high-definition maps from mobile mapping data for simulation testing applications in autonomous vehicle simulators. Master's thesis, National Cheng Kung University.

Chiang, K.W., Zeng, J.C., Tsai, M.L., Darweesh, H., Chen, P.X., Wang, C.K., 2022. Bending the Curve of HD Maps Production for Autonomous Vehicle Applications in Taiwan. IEEE Journal of Selected Topics in Applied Earth Observations and Remote Sensing, vol. 15, pp. 8346-8359. https://doi.org/10.1109/JSTARS.2022.3204306

Elghazaly, G., Frank, R., Harvey, S., Safko, S., 2023. High-Definition Maps: Comprehensive Survey, Challenges, and Future Perspectives. IEEE Open Journal of Intelligent Transportation Systems, 4, 527–550.

Gottschalk, S., 2000. Collision Queries using Oriented Bounding Boxes. PhD thesis, University of North Carolina at Chapel Hill.

He, K., Gkioxari, G., Dollár, P., Girshick, R., 2017. Mask R-CNN. Proc. IEEE Int. Conf. Comput. Vis. (ICCV), 2961–2969.

Jiang, H., 2017. Generation of Horizontally Curved Driving Lines for Autonomous Vehicles Using Mobile Laser Scanning Data. Master's thesis, University of Waterloo.

Lin, T.Y., Dollár, P., Girshick, R., He, K., Hariharan, B., Belongie, S., 2017. Feature pyramid networks for object detection. Proc. IEEE Conf. Comput. Vis. Pattern Recognit. (CVPR), 936–944.

Liu, C., Jiang, K., Chen, Z., Li, Y., Yang, D., 2024. High Definition Map Mapping and Update: A General Overview and Future Directions. arXiv preprint arXiv:2409.09726

Ma, L., Li, Y., Li, J., Wang, C., Wang, R., Chapman, M.A., 2019. Mobile Laser Scanned Point-Clouds for Road Object Detection and Extraction: A Review. Remote Sensing, 10(10), 1531. https://doi.org/10.3390/rs10101531

Otsu, N., 1979. A threshold selection method from gray-level histograms. IEEE Trans. Syst. Man Cybern., 9(1), 62–66.

Powers, D.M.W., 2011. Evaluation: From Precision, Recall and F-measure to ROC, Informedness, Markedness and Correlation. J. Mach. Learn. Technol., 2(1), 37–63.

Qi, C., Yi, L., Su, H., Guibas, L.J. 2017. PointNet++: Deep Hierarchical Feature Learning on Point Sets in a Metric Space. *ArXiv, abs/1706.02413*.

Ren, S., He, K., Girshick, R., Sun, J., 2015. Faster R-CNN: Towards real-time object detection with region proposal networks. Proc. NeurIPS, 91–99.

Rusu, R.B., 2010. Semantic 3D Object Maps for Everyday Manipulation in Human Living Environments. *KI - Künstliche Intelligenz, 24*, 345-348.

Wong, K., Gu, Y., Kamijo, S., 2021. Mapping for autonomous driving: Opportunities and challenges. IEEE Intell. Transp. Syst. Mag., 13(1), 91–106.

Yang, B., Fang, L., Li, J., 2013. Semi-automated extraction and delineation of 3D roads from mobile laser scanning point clouds. ISPRS J. Photogramm. Remote Sens., 79, 80–93.

Zeng, J.C., 2020. Automated Road-Elements Modelling and Centerline Generation for High-Definition Maps Utilizing 3D Point Cloud. Master’s thesis, National Cheng Kung University.

Zhang, W., Qi, J., Wan, P., Wang, H., Xie, D., Wang, X., Yan, G., 2016. An easy-to-use airborne LiDAR data filtering method based on cloth simulation. Remote Sens., 8(6), 501. doi.org/10.3390/rs8060501